Cytokine 155 (2022) 155898

Contents lists available at ScienceDirect

Cytokine

journal homepage: www.elsevier.com/locate/cytokine

# MicroRNA-23a-3p ameliorates acute kidney injury by targeting FKBP5 and NF-κB signaling in sepsis

Hui Xu, Zenggeng Wang *

*Department of Emergency, Jiangxi Provincial People's Hospital, Nanchang, Jiangxi 330006, PR China*

ARTICLE INFO

*Keywords:*
miR-23a-3p
FKBP prolyl isomerase 5
Nuclear factor kappaB
Acute kidney injury
Sepsis

ABSTRACT

Low miR-23a-3p expression in patients with acute kidney injury (AKI) or sepsis has been revealed. However, the specific role of miR-23a-3p in AKI remains unclear. Our study aimed to determine the function of miR-23a-3p in AKI. Exposure to lipopolysaccharide (LPS) was used to induce cell injury *in vitro*. Cecal ligation and puncture (CLP) surgery was used to establish an animal model of septic AKI. Bioinformatics analysis and a wide range of experiments, including RT-qPCR, luciferase reporter, western blot, ELISA, TUNEL, hematoxylin and eosin staining, and immunofluorescence assays were conducted. The experimental results revealed that LPS exposure induced the significant apoptosis and inflammatory response of HK-2 cells, and miR-23a-3p exhibited a low expression in LPS-exposed HK-2 cells. Functionally, miR-23a-3p overexpression inhibited cell apoptosis and release of inflammatory cytokines including interleukin (IL)-1β, IL-6 and IL-8. Mechanistically, miR-23a-3p bound to the FKBP prolyl isomerase 5 (FKBP5) 3′ untranslated region and negatively regulated its expression at mRNA and protein levels. Rescue assays indicated that FKBP5 overexpression reversed the influence of miR-23a-3p mimics on cell apoptosis and inflammatory response. Furthermore, miR-23a-3p overexpression attenuated the sepsis-induced impairment of renal function and the inflammatory response in mice with AKI. Finally, the knockdown of FKBP5 inactivated the nuclear factor kappaB (NF-κB) signaling by inactivating NF-κB nuclear translocation, and thereby inhibited the release of proinflammatory cytokines. Overall, our study demonstrates that miR-23a-3p ameliorates sepsis induced AKI by targeting FKBP5 and inactivating the NF-κB signaling, implying a potential therapeutic or diagnostic target for AKI.

## 1. Introduction

Sepsis, characterized by systemic inflammatory response, was reported to be the leading cause of mortality in intensive care units [1–3]. In particular, acute kidney injury (AKI) is a fatal complication that happens during the development of sepsis [4]. It has been estimated that severe sepsis is the cause for approximately 50% of AKI cases [5]. Recently, a number of researchers have explored the pathogenesis, progression and prognosis of septic AKI, while the pathophysiology of septic AKI remains elusive [6]. Thus, it is critical to elucidate the underlying mechanisms responsible for the pathogenesis of AKI and to identify potential effective markers for AKI diagnosis or treatment.

In recent years, it has been indicated that non-coding RNAs play critical roles in a number of diseases [7]. MicroRNAs, a subgroup of non-coding RNAs, are short and single stranded with approximately 22 nucleotides in length [8]. Despite the lack of protein-encoding ability, miRNAs are capable of combining with mRNA 3́ untranslated region (3́ UTR) to downregulate mRNA levels at the post-transcription level and thereby exert a marked effect on several cellular processes, like cell proliferation, apoptosis, differentiation, autophagy, and inflammation [9]. As an example, miR-218 was proposed to promote the osteogenic differentiation of fibroblast-like synovial cells via a ROBO/Slit pathway in rheumatoid arthritis [10]. Recently, miR-23a-3p has been extensively reported to be dysregulated in several tumors [11,12]. Importantly, miR-23a-3p inhibits the inflammatory response in diverse pathogeneses, including traumatic brain injury, insulin resistance and osteoarthritis [13–15]. Moreover, miR-23a-3p has been identified to display low level in blood samples collected from AKI patients [16] and in patients with sepsis [16]. Nevertheless, the specific role of miR-23a-3p in acute kidney injury (AKI) remains unclear.

The protein FKBP prolyl isomerase 5 (FKBP5), belonging to the immunophilin protein family, has been reported to participate in protein folding and trafficking [17,18]. Additionally, FKBP5, a cis–trans prolyl isomerase, was proposed to combine with the immunosuppressants

* Corresponding author at: Department of Emergency, Jiangxi Provincial People's Hospital, No. 152 Patriotic Way, Nanchang 330006, PR China.
*E-mail address:* wangzenggeng310@126.com (Z. Wang).

https://doi.org/10.1016/j.cyto.2022.155898
Received 17 December 2021; Received in revised form 12 April 2022; Accepted 23 April 2022
Available online 7 May 2022

FK506 or rapamycin [19–22]. Previously, FKBP5 was also identified to modulate inflammatory response in airway epithelial cells, Th2 cells and human fibroblasts [20,23,24]. However, the detailed role of FKBP5 in AKI is still unclear.

The NF-κB signaling was extensively reported to mediate the regulation of cell inflammatory response in sepsis-induced AKI [25–27]. In detail, the downregulation of tissue inhibitor of metalloproteinases inhibits the development of sepsis-induced AKI by regulating the NF-κB signaling [28]. Furthermore, Lidanpaidu prescription has been shown to inactivate NF-κB signaling to alleviate sepsis-induced AKI [29].

In the present study, an *in vitro* cell model and an animal model of sepsis-induced AKI were established to figure out the biological role and potential mechanisms of miR-23a-3p in sepsis-induced AKI. We concluded that miR-23a-3p attenuated AKI by targeting FKBP5 and NF-κB signaling in sepsis, which may provide a potential therapeutic or diagnostic target for patients with AKI.

## 2. Materials and methods

### 2.1. Septic patients and healthy controls

Eighteen septic plasma samples were collected from eighteen septic patients who were admitted to intensive care unit at the Jiangxi Provincial People's Hospital (Nanchang, Jiangxi), and eight normal control plasma samples were collected from eight healthy volunteers. Patients were diagnosed with sepsis according to the American College of Chest Physicians/Society of Critical Care Medicine consensus definition [30]. The study was approved by the Ethic Committee of the Jiangxi Provincial People's Hospital (No. 2022-021; Nanchang, Jiangxi). The ethical document was provided as a supplemental file.

### 2.2. Bioinformatics analysis

The present study used the starBase tool (starBase: https://starbase.sysu.edu.cn/) to reveal the potential targets of miR-23a-3p. Predicted by PITA, RNA22, miRanda and TargetScan programs in starBase, 6 mRNAs including CAMTA1, PHLDA1, TK2, FKBP5, TNFAIP3 and PPP2R5E were identified.

### 2.3. Cells and cell treatment

HK-2 cells (American Type Culture Collection, Manassas, USA) were cultured in Dulbecco's modified Eagle's medium (DMEM; Thermo Fisher Scientific, Inc. USA) with 10% fetal bovine serum (FBS; Gibco), streptomycin (100 μg/ml) and penicillin (100 U/ml, Sigma-Aldrich; USA) in a humidified atmosphere with 5% $CO_2$ at 37 °C. For cell treatment, the HK-2 cells were stimulated by 100 ng/ml [31] of lipopolysaccharide (LPS) for 24 h to mimic cell injury, and cells treated with the same dose of cell culture medium served as the controls (Con).

### 2.4. Cell transfection

For cell transfection, 50 nmol/l of miR-23a-3p mimics (miR-23a-3p, GenePharma, Shanghai, China) were applied for the overexpression of miR-23a-3p, and NC mimics (50 nmol/l, GenePharma) served as the negative controls. The full length of FKBP5 was inserted into the pcDNA3.1 vector (500 ng/well, GenePharma) to overexpress FKBP5 with empty pcDNA3.1 serving as a control. sh-FKBP5 (20 nmol/l) was used to knock down FKBP5 expression. Plasmids were transfected into cells using Lipofectamine 2000 reagent (Thermo Fisher Scientific) under the manufacturer's instruction. Forty-eight hours after transfection, subsequent experiments were conducted.

### 2.5. Establishment of a mouse model of sepsis

A total of 75 C57BL/6 mice (male, 6–8 weeks old, weighing 20–22 g) were purchased from Vital River Co. ltd. All mice were raised independently with 50% humidity at 20–25 °C, and randomly divided into 4 groups as follows: The sham-operated (sham) group (n = 15), sham + AAV-miR-23a-3p group (n = 15), the cecal ligation and puncture (CLP) group (n = 15), the CLP + AAV-NC group (n = 15) and the CLP + AAV-miR-23a-3p group (n = 15). CLP surgery was used to the establish the animal model of sepsis as previously described [32]. At first, mice in the different groups were anesthetized by the inhalation of isoflurane. Following oral intubation, the mice were anesthetized with isoflurane (5% for induction and 2% for maintenance) and mechanically ventilated with 20% oxygen and 80% air. The abdomen of the mice was then wiped with 70% isopropanol after shaving, and an incision (1 to 2 cm) was made at the midline abdomen. Simultaneously, after exteriorizing the cecum, a sterile silk suture was used for ligation (1 cm from the tip), and a 20-gauge needle was used for puncture twice. After squeezing minimal fecal material out from the cecum, the cecum was returned to the abdominal cavity. Finally, the incision was sutured with auto-clips and cleaned by povidone-iodine (betadine). The sham-operated mice received similar treatment but without CLP. All mice were sacrificed 24 h after CLP or sham operation by cervical dislocation. Mouse kidneys were dissected for the following assays. All experimental procedures were approved by the National Institutes of Health Guidelines for the Care and Use of Laboratory Animals. Ethics approval for the animal studies has been obtained from the Ethics Committee of the Jiangxi Provincial People's Hospital.

### 2.6. Injection of adeno-associated virus (AAV)

AAV (serotype 2, Vigene Biosciences, shanghai, China) containing the sequences of miR-23a-3p and empty AAV were injected ($10^{12}$ vg/ml) via the tail vein into mice (n = 15 in each group) at 21 days prior to CLP surgery.

### 2.7. Measurement of renal function

Venous blood (5 ml) was collected via tail vein. Serum creatinine (SCr) levels were detected using a creatinine assay kit (BioAssay Systems, LLC), and the blood urea nitrogen (BUN) concentration was determined with a Hitachi 7060 automatic biochemistry analyzer (Hitachi, ltd.).

### 2.8. Reverse transcription-quantitative polymerase chain reaction (RT-qPCR)

TRIzol Reagent (Thermo Fisher Scientific) was utilized for the extraction of RNA from HK-2 cells and renal tissues. A RevertAid First Strand cDNA Synthesis kit (K1622; Thermo Fisher Scientific) and a TaqMan advanced miRNA cDNA synthesis kit (A28007; Applied Biosystems, USA) were used for reverse transcription. The qPCR was performed with the SYBR-Green PCR Master Mix kit (4367659; Applied Biosystems) or the TaqMan miRNA assay kit (4440887; Applied Biosystems). The RNA levels were calculated with the $2^{-\Delta\Delta Cq}$ method [33]. GAPDH and U6 functioned as the internal controls. Relative PCR primer sequences are provided in Table SI.

### 2.9. Histological analysis

Renal tissues were isolated from the mice in sham and CLP groups. After being fixed with 4% paraformaldehyde, the renal tissues were embedded, sliced into sections (4 μm), and stained with hematoxylin (5 min) and eosin (2 min) at room temperature. Finally, the pathological changes were observed under a light microscope (Leica DM 6000 B; Leica Microsystems GmbH). The degree of kidney damage was determined using the following criteria: 0, Normal; 1, area of damage <25% of tubules; 2, damage involving 25–50% of tubules; 3, damage involving 50–75% of tubules; and 4, damage involving 75–100% of tubules.

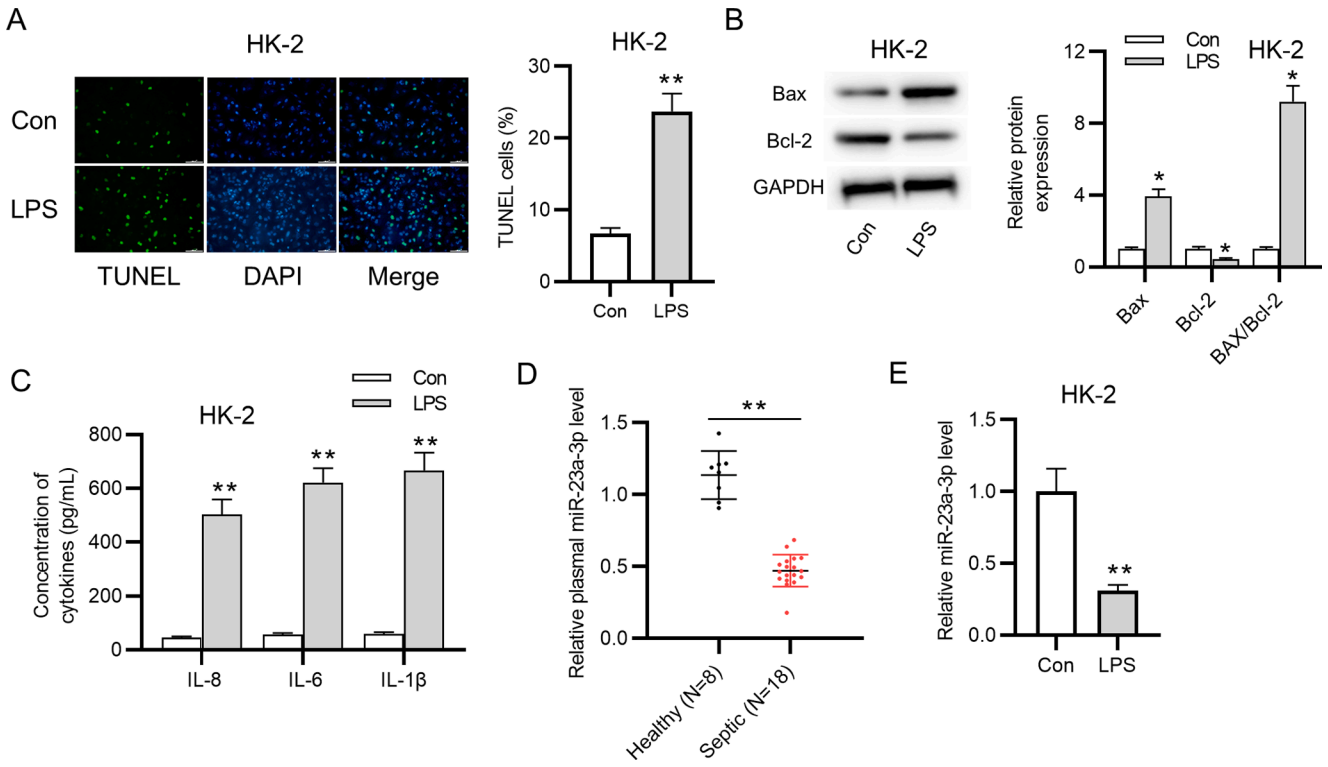


**Fig. 1.** LPS induced cell apoptosis, inflammatory response and miR-23a-3p downregulation. (A) TUNEL assay was used to measure cell apoptosis. (B) Bax and Bcl-2 protein levels in HK-2 cells were examined by western blot analysis. (C) Contents of IL-8, IL-6 and IL-1β in the supernatant of HK-2 cells were detected by ELISA in HK-2 cells. (D) RT-qPCR was applied to detect the miR-23a-3p levels in plasma from 18 septic patients and 8 healthy individuals. (E) RT-qPCR was applied to detect the miR-23a-3p level in HK-2 cells. *$p < 0.05$, **$p < 0.01$, vs control.

### 2.10. TUNEL staining

TUNEL staining was conducted to analyze the apoptosis of HK-2 cells using the *In Situ* Cell Death Detection kit (11684817910; Roche Diagnostics). Following fixation in 4% PFA (Sigma-Aldrich), the HK-2 cells were stained for 60 min at 37 °C using TUNEL reaction mixture. Cell nuclei were dyed using DAPI (1:100; Sigma-Aldrich) for 10 min at room temperature. Images were observed using a light microscope (BX53; Olympus Corporation).

### 2.11. Enzyme-linked immunosorbent assay (ELISA)

After indicated treatment, mouse serum or supernatants of HK-2 cells were used for ELISA. Interleukin (IL)-6, IL-8, and IL-1β levels in the supernatants of HK-2 cells were detected using human IL-6 ELISA kit (ab178013, Abcam), human IL-8 ELISA kit (ab214030, Abcam), and human IL-1β ELISA kit (ab214025, Abcam), respectively. The levels of above three cytokines in mouse serum were evaluated utilizing mouse IL-6 ELISA kit (ab100713, Abcam), mouse IL-8 (CXCL-15) ELISA kit (ab193720, Abcam), and mouse IL-1β ELISA kit (ab197742, Abcam), respectively, as per the manufacturer's instructions. For detecting the effects of NF-κB inhibition on IL-6, IL-8 and IL-1β proteins, cells were treated with 0.5 μmol/l of 4-N-[2-(4-phenoxyphenyl)ethyl]quinazoline-4,6-diamine (QNZ, an inhibitor of NF-κB; SelleckChem) for 24 h.

### 2.12. Protein extracts from cytoplasm and nucleus

HK-2 cell suspensions were prepared by Trypsin-EDTA treatment. The protein samples in cytoplasm and nucleus of the HK-2 cells were extracted using NE-PER™ nuclear and cytoplasmic extraction reagents (78833; Thermo Fisher Scientific) following the manufacturer's protocols.

### 2.13. Western blot analysis

HK-2 cells or renal tissues were lysed with lysis buffer containing protease inhibitors. The protein concentration was determined using a BCA Protein Assay kit (Beijing Solarbio Science & Technology). Protein (30 μg protein per lane) from each sample was resolved by 12% SDS-PAGE and then transferred onto PVDF membranes. After being blocked with 5% skim milk for 1 h at 37 °C, the membranes were incubated with primary antibodies against Bcl-2 (ab182858, 1/2,000), Bax (ab32503, 1/1,000), FKBP5 (ab126715, 1/1,000), p50 (ab32360, 1/5,000), p-p65 (ab76302, 1/1,000), p65 (ab32536, 1/2,000), p-IκBα (ab133462, 1/10,000), IκBα (ab32518, 1/1,000), Lamin B (ab133741, 1/1,000) and GAPDH (ab9485, 1/2,500) at 4 °C overnight. The membranes were subsequently incubated using secondary antibodies (ab205718, 1/2,000) at room temperature for 2 h. All the antibodies were purchased from Abcam. Finally, proteins were visualized via an enhanced chemiluminescence (Beyotime Institute of Biotechnology) and quantified with the ImageJ software (version 1.38X; National Institutes of Health).

### 2.14. Luciferase reporter assay

The binding site between miR-23a-3p on FKBP5 was predicted by the TargetScan website (https://www.targetscan.org/vert_71/). The 3′ UTR of FKBP5 complementary to miR-23a-3p was sub-cloned into pmirGLO plasmids (Promega, USA) to construct the pmirGLO-FKBP5-Wt plasmids. The mutated 3′ UTR of FKBP5 was sub-cloned into pmirGLO plasmids to construct the pmirGLO-FKBP5-Mut plasmids. HK-2 cells were co-transfected with wild-type or mutant pmirGLO dual-luciferase vector FKBP5 (1 μg) together with 25 nM of miR-23a-3p mimics or NC mimics using Lipofectamine 2000 in 24-well plates. Luciferase activity was detected 48 h after vector transfection using dual luciferase reporter assay system (Promega).

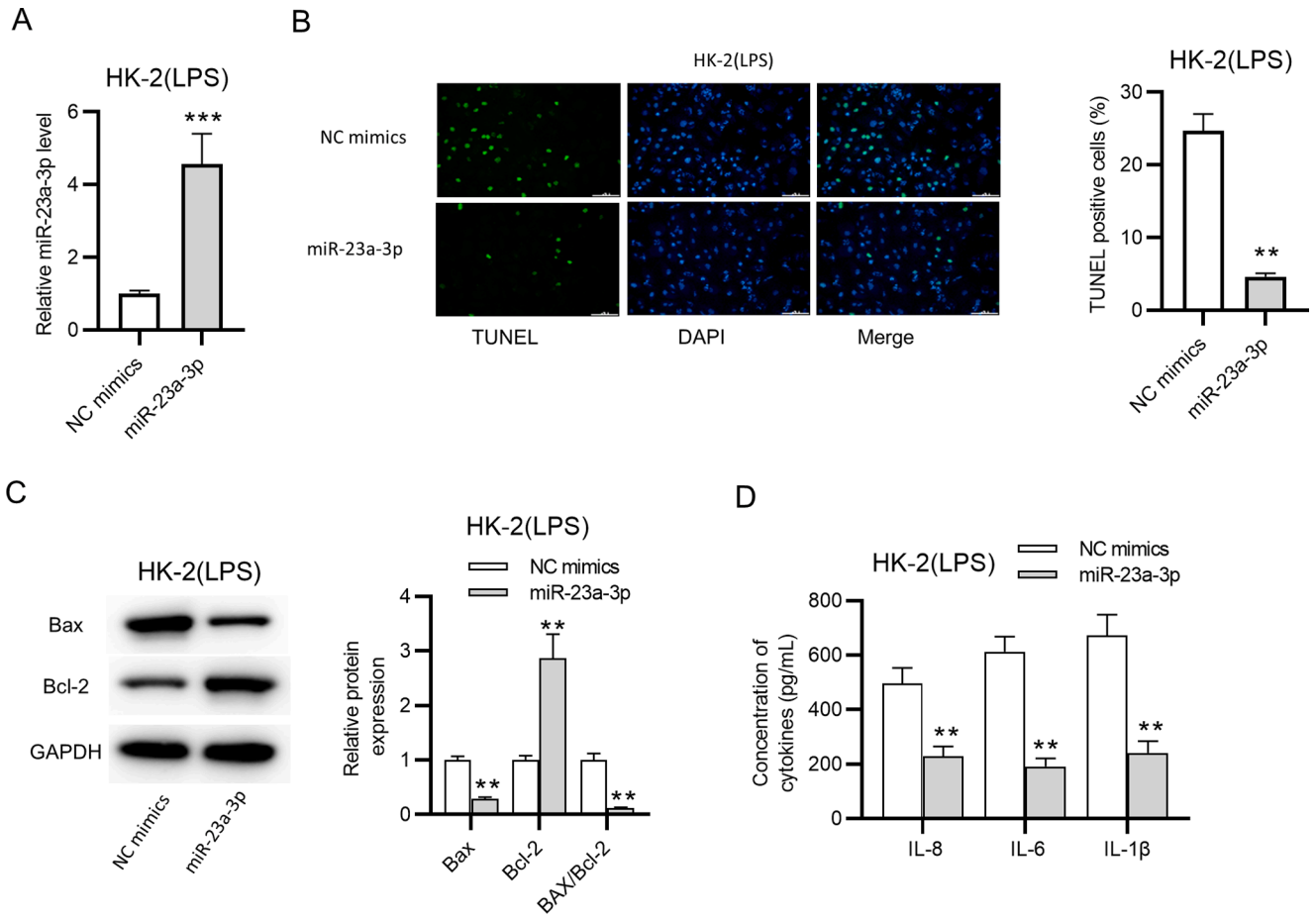


**Fig. 2.** miR-23a-3p hinders cell apoptosis and inflammation of LPS-exposed HK-2 cells. (A) The overexpression efficiency of miR-23a-3p mimics in LPS-exposed cells. (B) TUNEL assay was performed to measure the apoptosis of LPS-exposed cells. (C) Western blot was used to determine Bax and Bcl-2 protein levels in LPS-exposed cells. (D) Accumulation of IL-8, IL-6 and IL-1β in the supernatants of LPS-stimulated HK-2 cells were detected by ELISA in LPS-exposed cells. $^{**}p < 0.01$, $^{***}p < 0.001$, vs NC mimics.

### *2.15. RNA immunoprecipitation (RIP) assay*

A Magna RIP RNA-Binding Protein Immunoprecipitation kit (17-700; EMD Millipore) was used for RIP assay. Cells were incubated with radioimmunoprecipitation assay lysis buffer. The cell lysates were then probed with magnetic beads conjugated with anti-Ago2 antibody (ab186733, 1/30, Abcam) or control anti-IgG antibody (ab6715, 1/100, Abcam). The cell lysates were then treated with 150 μl of proteinase K buffer at 55 °C for 30 min to digest the protein. The expression of miR-23a-3p and FKBP5 in precipitates of anti-Ago2 or anti-IgG was measured by RT-qPCR.

### *2.16. Immunofluorescence (IF) staining*

HK-2 cells were seeded in 6-well plates and fixed with 4% paraformaldehyde. Subsequently, 0.5% Triton X-100 was applied to permeabilize cell for 10 min at room temperature. Hereafter, the cells were blocked in PBST containing 5% BSA (Amersco) for 1 h, and then incubated with primary antibody anti-NF-κB (ab16502, 1/100, Abcam) overnight at 4 °C. Subsequently, fluorochrome-labeled anti-rabbit secondary antibody (ab6717, 1/1,000, Abcam) was added for 1 h of incubation at room temperature. DAPI (Beyotime) was applied to stain the nucleus. Images were observed under a fluorescence microscope (Nikon Corporation) and analyzed using Adobe Photoshop 6.0 software.

### *2.17. Statistical analysis*

Statistical analysis was performed with SPSS software (version 17.0). Data were shown as the means ± SD (standard deviation). The unpaired Student's *t*-test was used for comparison between 2 groups. One-way analysis of variance followed by Tukey's *post hoc* test was applied for the comparisons of >2 groups. P-value <0.05 was considered to possess a statistical significance.

## 3. Results

### *3.1. miR-23a-3p level is downregulated in LPS-exposed cells*

A previous study identified that serum miR-23a-3p level was decreased in sepsis-induced AKI patients [16]. To further investigate the function of miR-23a-3p in AKI, we established a cell model of sepsis by exposing HK-2 cells to LPS. As shown in Fig. 1A, LPS stimulation significantly promoted cell apoptosis. Furthermore, LPS exposure elevated Bax protein level but reduced Bcl-2 protein level (Fig. 1B). Moreover, the addition of LPS increased the accumulation of IL-6, IL-8 and IL-1β in the supernatant of HK-2 cells (Fig. 1C). Plasma miR-23a-3p levels were lower in 18 septic patients than 8 healthy individuals (Fig. 1D). RT-qPCR analysis also demonstrated that LPS exposure decreased miR-23a-3p expression in HK-2 cells (Fig. 1E).

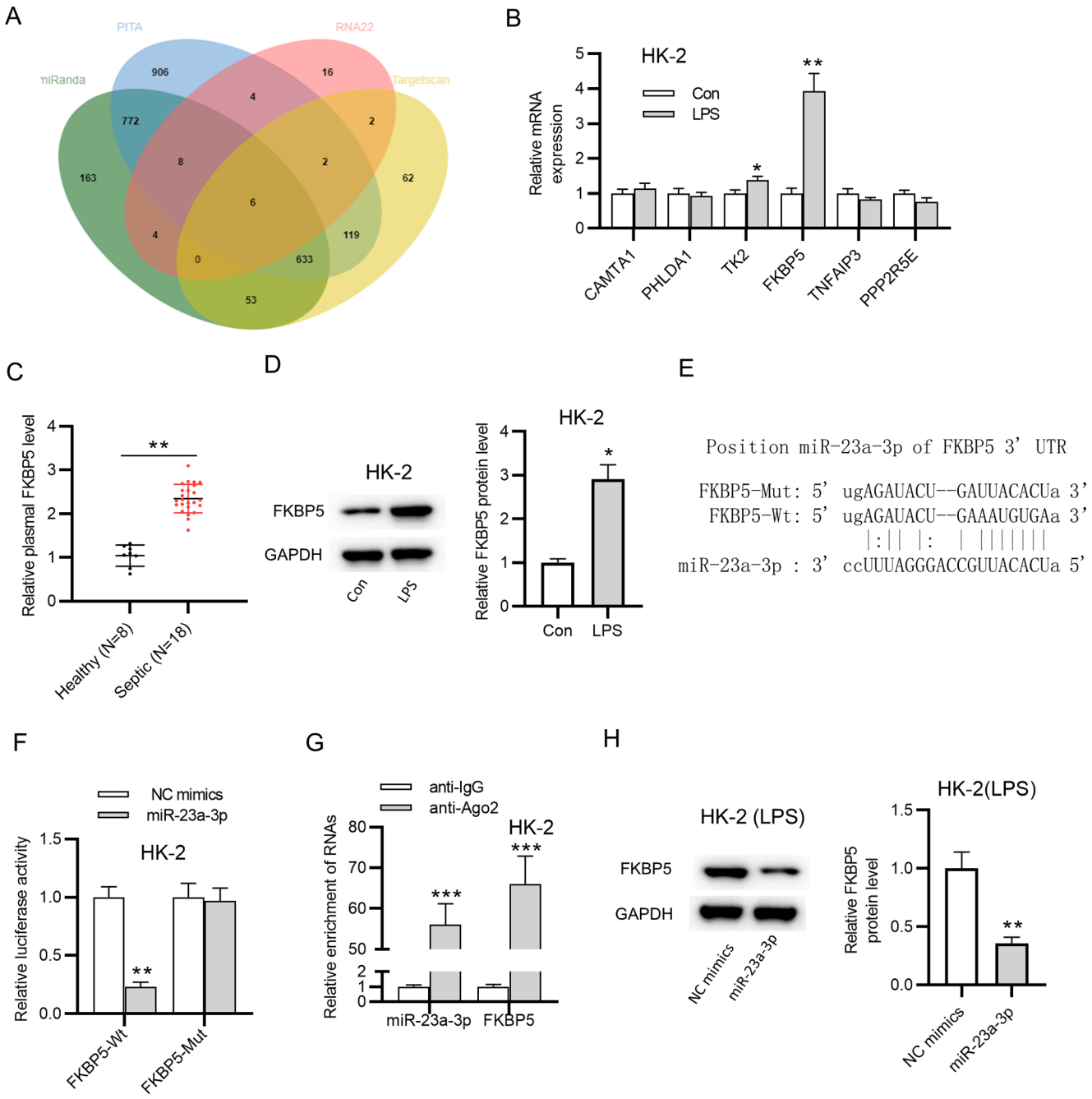


**Fig. 3.** miR-23a-3p can directly bind with the FKBP5 3́ UTR. (A) Venn diagram showing the mRNAs harboring the binding site on miR-23a-3p. (B) RT-qPCR analysis was performed to measure the levels of candidate mRNAs in HK-2 cells exposed to LPS or not. (C) RT-qPCR was applied to detect the FKBP5 levels in plasma from 18 septic patients and 8 healthy individuals. (D) Western blot analysis was used to determine the protein level of FKBP5 in HK-2 cells exposed to LPS or not. (E) Binding sequences of miR-23a-3p on position 667–674 of FKBP5 3′ UTR. (F) Luciferase reporter assay was applied to examine the luciferase activities of wild-type or mutant pmirGLO-FKBP5. (G) Relative enrichment of miR-23a-3p and FKBP5 in IgG and Ago2 precipitated products. (H) Western blot analysis was used to determine the protein level of FKBP5 in LPS-exposed HK-2 cells in the context of miR-23a-3p overexpression. *$p < 0.05$, **$p < 0.01$, ***$p < 0.001$ vs respective controls.

### 3.2. *miR-23a-3p hinders cell apoptosis and the inflammatory response of LPS-stimulated HK-2 cells*

We then evaluated the effects of miR-23a-3p exerted on HK-2 cell apoptosis and inflammation. First, miR-23a-3p levels were effectively overexpressed by transfection of miR-23a-3p mimics (Fig. 2A). Moreover, TUNEL assay demonstrated that number of TUNEL-positive cells was decreased by miR-23a-3p overexpression (Fig. 2B). Additionally, miR-23a-3p mimics reduced the Bax protein level and increased the Bcl-2 protein level (Fig. 2C). In addition, the contents of IL-8, IL-6 and IL-1β in the supernatants of LPS-exposed HK-2 cells were significantly downregulated by miR-23a-3p overexpression (Fig. 2D).

### 3.3. *miR-23a-3p directly binds with the FKBP5 3́ UTR*

Emerging evidence suggests that miR-23a-3p can bind with the mRNA 3́ UTR to inhibit its mRNA and protein levels [34,35]. It was thus hypothesized that miR-23a-3p also acts in this pattern in AKI. Using bioinformatics analysis, 6 potential target mRNAs were found and are shown in Fig. 3A (conditions: predicted by PITA, RNA22, miRanda and TargetScan). Additionally, RT-qPCR results indicated that only FKBP5 exhibited the most evident upregulation in LPS-stimulated HK-2 cells

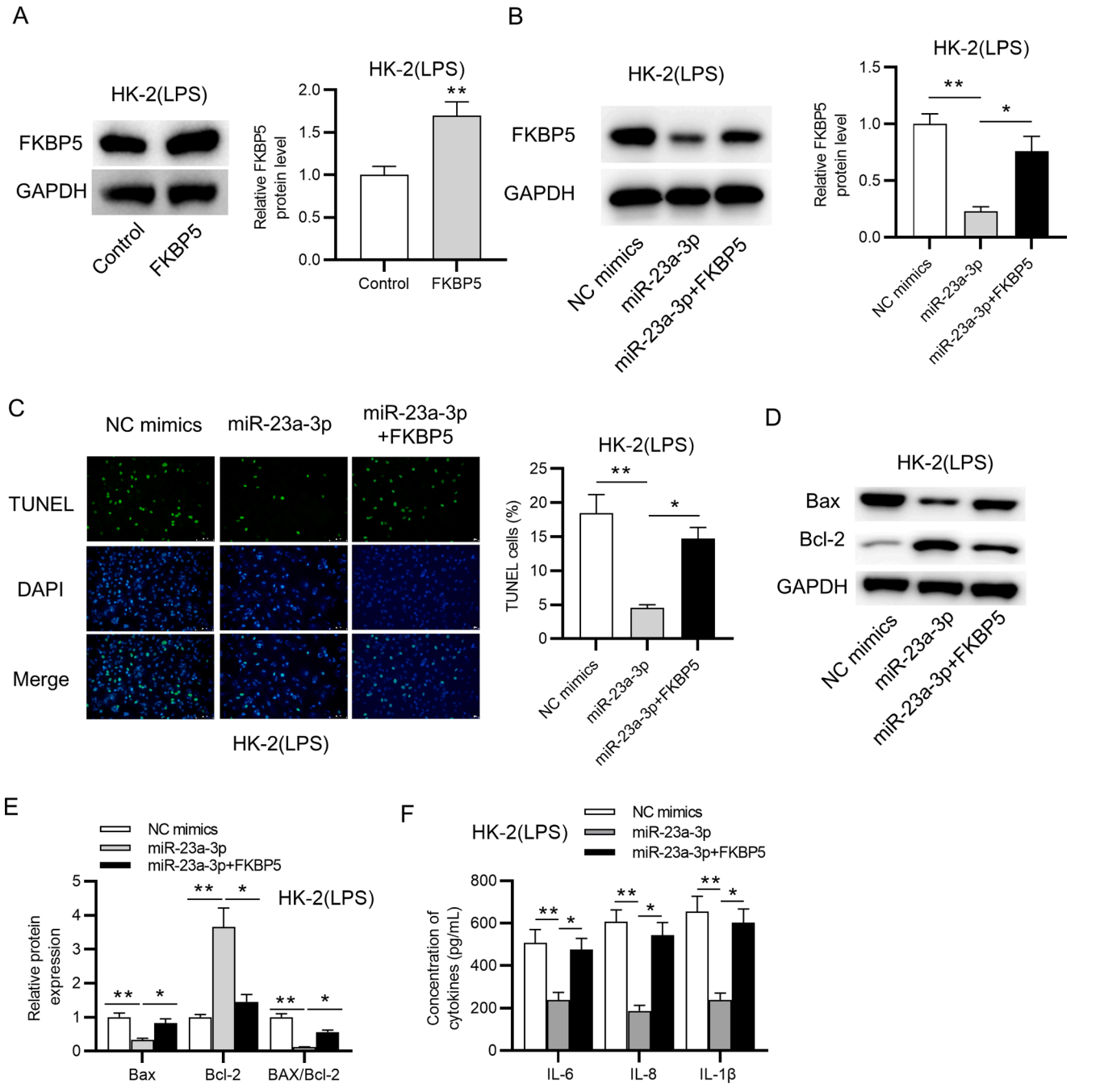


**Fig. 4.** miR-23a-3p regulates cell apoptosis and inflammation via targeting FKBP5. (A) The overexpression efficacy of pcDNA3.1/FKBP5 in LPS-exposed cells. (B) Western blot analysis of FKBP5 protein levels in NC mimics, miR-23a-3p mimics, miR-23a-3p mimics + FKBP5 groups in LPS-exposed cells. (C) TUNEL assay was used to measure the apoptosis of LPS-exposed cells in the different groups. (D and E) Bax and Bcl-2 protein levels in the different groups. (F) ELISA was used to detect the contents of IL-8, IL-6 and IL-1β in the supernatants of LPS-stimulated HK-2 cells in above three groups. *$p < 0.05$, **$p < 0.01$ vs respective controls.

among these mRNAs (Fig. 3B). Plasma FKBP5 levels were higher in 18 septic patients than 8 healthy individuals (Fig. 3C). Likewise, the FKBP5 protein levels were increased in the LPS-stimulated HK-2 cells (Fig. 3D). According to the prediction of the TargetScan website, the binding position of miR-23a-3p on the FKBP5 3́ UTR is presented in Fig. 3E. Based on luciferase reporter assay, miR-23a-3p overexpression attenuated the luciferase activity of wild-type pmirGLO-FKBP5, whereas the luciferase activity of mutant pmirGLO-FKBP5 was not significantly altered (Fig. 3F). In addition, miR-23a-3p and FKBP5 were significantly enriched in Ago2 precipitated products according to RNA immunoprecipitation assay (Fig. 3G). Finally, miR-23a-3p also reduced the FKBP5 protein level in the LPS-stimulated HK-2 cells (Fig. 3H).

### *3.4. miR-23a-3p regulates cell apoptosis and the inflammatory response by targeting FKBP5*

To explore whether miR-23a-3p affects cell apoptosis and inflammation by targeting FKBP5 in HK-2 cells, rescue assays were designed and performed. The protein level of FKBP5 was significantly overexpressed by transfection with pcDNA3.1/FKBP5 (Fig. 4A). The overexpression of FKBP5 significantly reversed the suppressive effect of miR-23a-3p on FKBP5 protein level (Fig. 4B). Subsequently, cell apoptosis was detected by TUNEL assay. It was found that FKBP5 overexpression counteracted the inhibitory effect of miR-23a-3p mimics on cell apoptosis (Fig. 4C). Furthermore, western blot analysis revealed that the

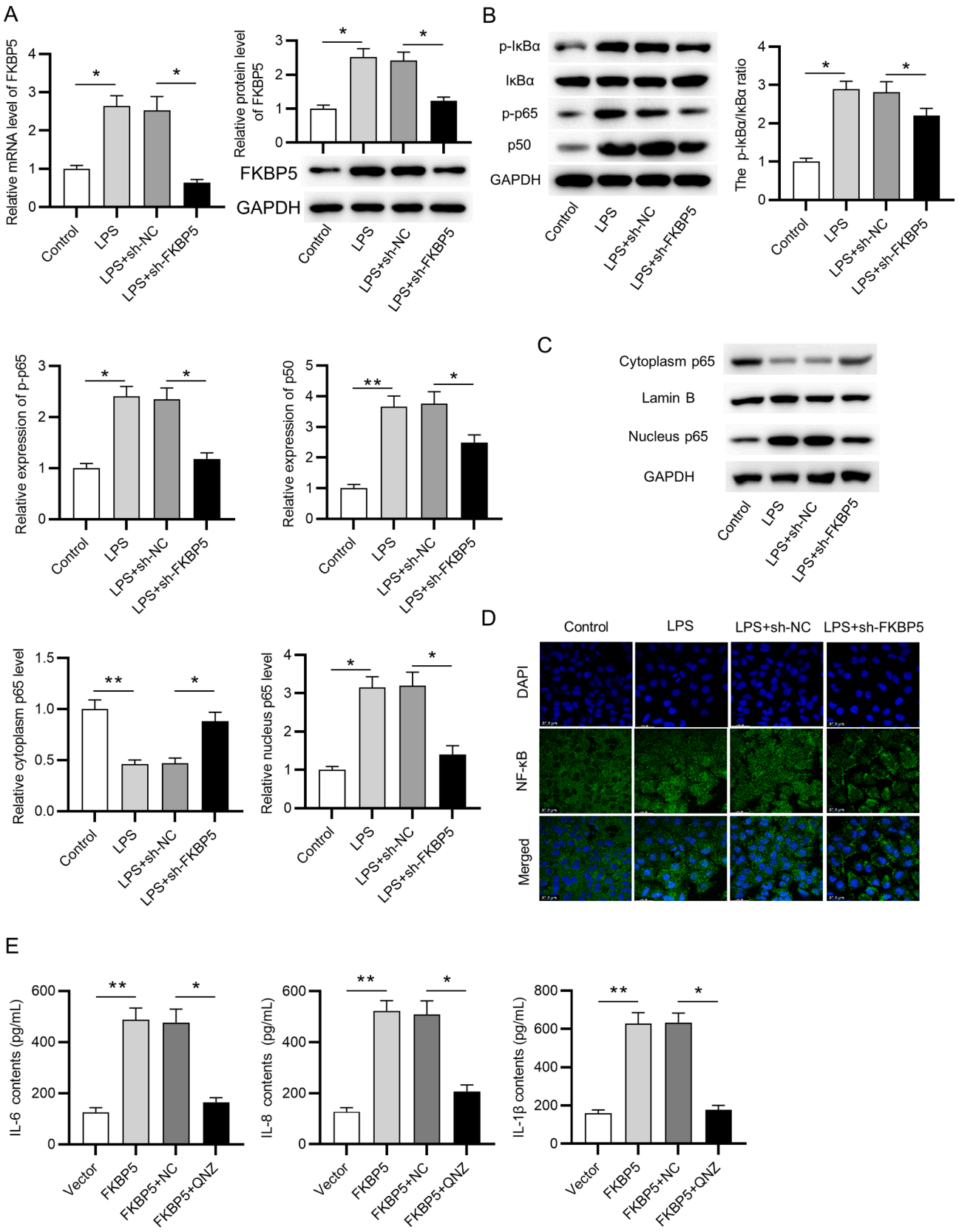


**Fig. 5.** FKBP5 exerts effects on the cell inflammatory response by targeting the NF-κB signaling pathway. (A) Knockdown efficacy of FKBP5 was explored by RT-qPCR and western blot analysis. (B) Effects of sh-FKBP5 on p50, phosphorylated p65, phosphorylated IκBα, and IκBα levels in LPS-exposed HK-2 cells were detected by western blotting. (C) Effects of sh-FKBP5 on cytoplasmatic p65 and nuclear p65 levels in LPS-exposed HK-2 cells. (D) Immunofluorescence assay showed the nuclear translocation of NF-κB in LPS-exposed HK-2 cells. (E) The contents of IL-8, IL-6 and IL-1β in the supernatants of HK-2 cells were examined by ELISA in the indicated groups. $^{*}p < 0.05$, $^{**}p < 0.01$ vs respective controls.

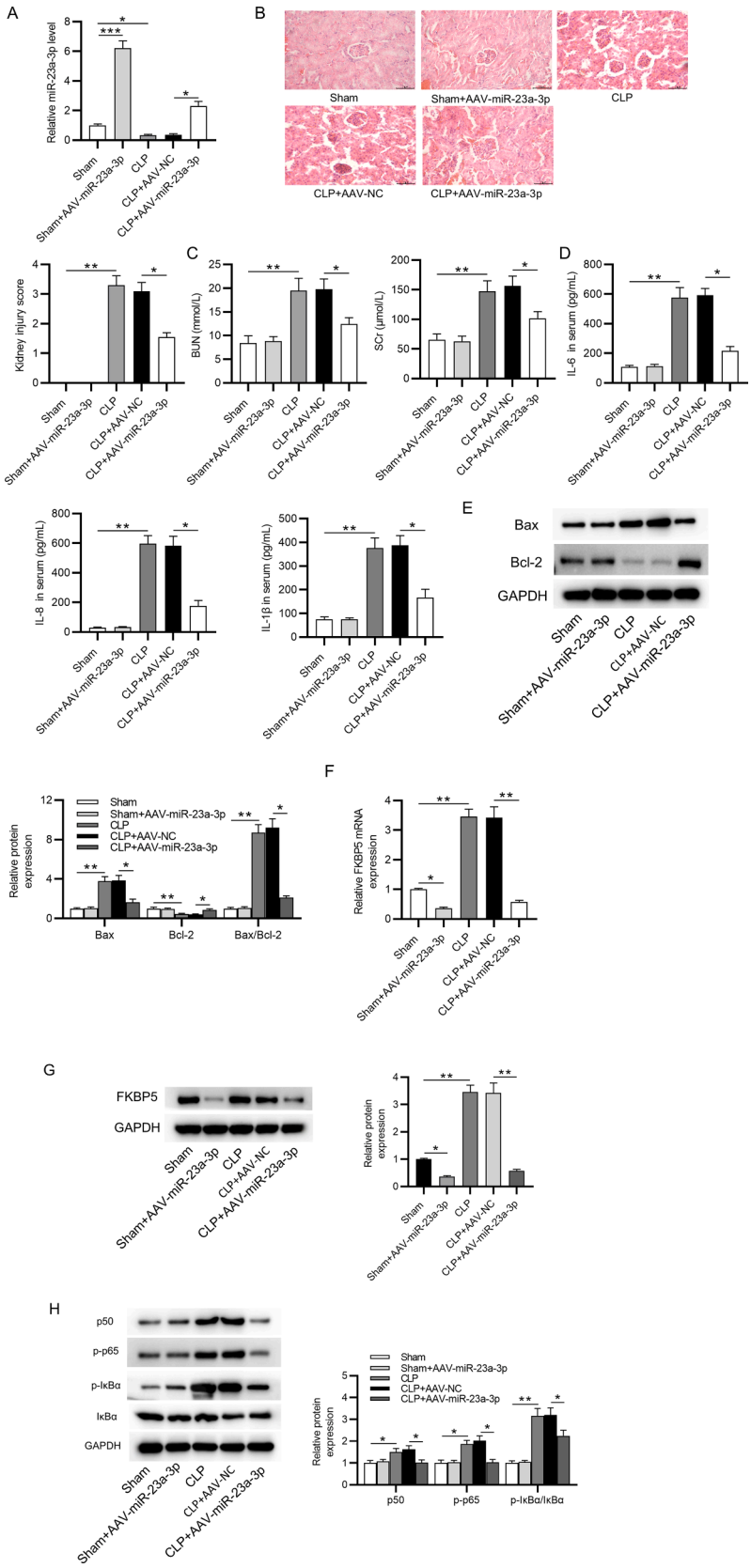


**Fig. 6.** miR-23a-3p overexpression alleviates sepsis-induced AKI in mice. (A) RT-qPCR analysis was conducted to evaluate the overexpression efficiency of miR-23a-3p mimics in mice (n = 15/group). (B) H&E staining was used to analyze the histological changes of the kidney tissues (n = 15/group). (C) Statistical analysis detected the BUN and serum creatinine (n = 15/group) levels. (D) The serum contents of IL-8, IL-6 and IL-1β were examined by ELISA in mice (n = 15/group). (E) The Bax and Bcl-2 protein levels in renal tissues were detected by western blot analysis (n = 15/group). (F-G) RT-PCR and western blot analyses were performed to determine FKBP5 mRNA and protein levels in renal tissues of mice (n = 15/group). (H) Protein levels of p50, phosphorylated p65, phosphorylated IκBα, and IκBα in renal tissues were detected by western blot analysis (n = 15/group). *p < 0.05, **p < 0.01, ***p < 0.001. BUN, blood urea nitrogen; SCr, serum creatinine.

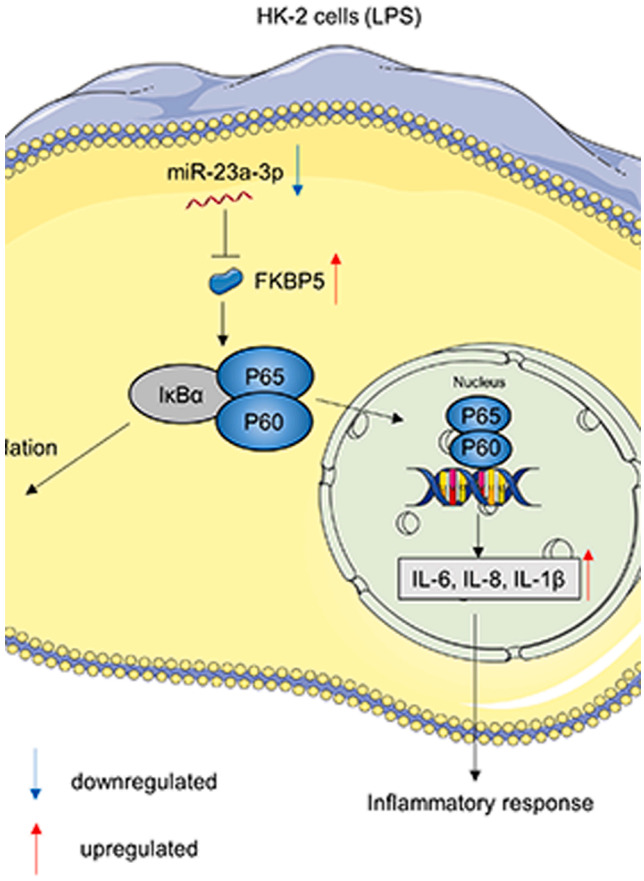


**Fig. 7.** A schematic diagram to illustrate the mechanism mediated by miR-23a-3p in LPS-stimulated HK-2 cells.

miR-23a-3p mimic-induced decrease in the Bax protein level and the increase in Bcl-2 protein level were neutralized by FKBP5 overexpression (Fig. 4D and E). In addition, the inhibitory influence of miR-23a-3p on the IL-8, IL-6 and IL-1β contents in the supernatants of LPS-stimulated HK-2 cells was abrogated by FKBP5 overexpression (Fig. 4F).

### *3.5. FKBP5 facilitates cell inflammatory response by targeting NF-κB signaling*

Previously, FKBP5 was indicated to be involved in the NF-κB signaling-activated inflammatory response [36]. We then explored the correlation between FKBP5 and NF-κB signaling in HK-2 cells. The mRNA and protein levels of FKBP5 were increased by LPS exposure and then knocked down by transfection with sh-FKBP5 (Fig. 5A). Moreover, western blot analysis indicated that LPS-induced the increase in the p-IκBα/IκBα ratio, p50 and phosphorylated p65 protein levels was suppressed by the knockdown of FKBP5 (Fig. 5B). Additionally, the increased nuclear p65 protein level and the decreased cytoplasmic p65 protein level resulting from LPS exposure were also neutralized by FKBP5 inhibition (Fig. 5C). Similarly, immunofluorescence assay revealed that the LPS-induced translocation of NF-κB was offset by FKBP5 inhibition (Fig. 5D). Finally, the increase in cytokine contents arising from FKBP5 overexpression in the supernatants of HK-2 cells was abrogated by treatment with QNZ (Fig. 5E).

### *3.6. miR-23a-3p overexpression alleviates sepsis-induced AKI in mice*

To further clarify the function of miR-23a-3p in sepsis-induced AKI, an animal model of AKI was established by performing CLP surgery on mice. To begin with, RT-qPCR revealed that the miR-23a-3p level was effectively overexpressed by the injection of AAV-miR-23a-3p to sham-operated mice (Fig. 6A). Additionally, miR-23a-3p level was greatly reduced after CLP surgery compared with that in the sham group (Fig. 6A). The injection of AAV-miR-23a-3p to mice in CLP group successfully upregulated miR-23a-3p expression (Fig. 6A). Furthermore, H&E staining assay indicated that miR-23a-3p overexpression alleviated kidney damage resulting from CLP surgery (Fig. 6B). Furthermore, the concentrations of BUN and SCr increased by CLP were decreased by the injection of AAV-miR-23a-3p (Fig. 6C). ELISA revealed that serum IL-8, IL-6 and IL-1β levels were reduced by miR-23a-3p overexpression in mice subjected to CLP (Fig. 6D). In response to miR-23a-3p overexpression, Bax protein levels were also reduced, while Bcl-2 protein levels were increased (Fig. 6E). FKBP5 expression in the mouse model was also detected. PCR analysis and western blot analyses revealed that FKBP5 mRNA and protein levels were upregulated in mice received CLP surgery (Fig. 6F and G). Additionally, FKBP5 levels were downregulated by miR-23a-3p both in sham-operated mice or AKI model mice (Fig. 6F and G). Moreover, Fig. 6H revealed that the ratio of p-IκBα/IκBα, p50 and phosphorylated p65 protein levels were higher in the renal tissues of mice in the CLP group than that in the sham group. Mice injected with AAV-miR-23a-3p showed decreased ratio of renal p-IκBα/IκBα, p50 and phosphorylated p65 protein levels (Fig. 6H).

### *3.7. miR-23-3p inhibits HK-2 cell apoptosis and inflammation by targeting FKBP5 to inactivate the NF-κB signaling*

As shown by the diagram Fig. 7, miR-23a-3p was downregulated in HK-2 cells after LPS stimulation while FKBP5 level was upregulated. FKBP5 promotes the phosphorylation of IκBα, leading to proteasomal degradation and the releasing of NF-κB. The nuclear translocation of p65 and p50 increased the levels of cytokines, thereby promoting HK-2 cell inflammation. miR-23a-3p targets FKBP5 to inactivate the NF-κB signaling and thus alleviates HK-2 cell apoptosis and inflammatory response.

## 4. Discussion

AKI, a common and severe complication during the development of sepsis, is characterized by insufficient blood filtration and impaired urine production [37,38]. With high morbidity and mortality, sepsis-induced AKI is a serious threat to human health [37,39]. Although modern therapies, including continuous renal replacement therapy, hemodialysis, peritoneal dialysis and sustained low-efficiency dialysis are used for the treatment of patients with AKI, the prognosis of such patients remains poor [40]. miRNAs have been identified to serve as biomarkers in AKI. For instance, miRNA-20a inhibits LPS-induced injury to HK-2 cells by targeting CXCL12 via NF-κB and ERK1/2 signaling in AKI [41]. Additionally, exosomal miR-21 has been reported to exert protective effects on kidney during sepsis progression [42]. Moreover, miR-218-5p alleviates AKI by targeting heme oxygenase-1 in sepsis [43]. Recently, miR-23a-3p downregulation has been identified in the serum of AKI patients [16]. In our study, miR-23a-3p exhibited relatively low levels in LPS-exposed HK-2 cells. MiR-23a-3p overexpression inhibited cell apoptosis and inflammatory response under LPS treatment. Furthermore, miR-23a-3p overexpression alleviated histological alterations, renal dysfunction, inflammatory response, and cell apoptosis in AKI mouse.

Mechanistically, miR-23a-3p has been proposed to inhibit mRNA translation by binding to the 3′ UTR of mRNAs. For example, miR-23a-3p binds with the 3′ UTR of KLF3 to regulate melanoma progression [44]. Moreover, miR-23a-3p has been reported to bind with SNAP-25 3′ UTR region to modulate Alzheimer's disease [45]. Likewise, in the present study, it was revealed that miR-23a-3p interacted with FKBP5 3′ UTR and inhibited its mRNA expression. Furthermore, miR-23a-3p negatively regulated the FKBP5 protein levels.

Previously, FKBP5 was reported to participate in the inflammatory

response [36,46,47]. Additionally, the dysregulation of FKBP5 is involved in the activation of NF-κB signaling [36]. In the present study, rescue assays revealed that the inhibitory effect of miR-23a-3p mimics on cell apoptosis and inflammatory response was reversed by the overexpression of miR-23a-3p and FKBP5. Finally, it was demonstrated that the knockdown of FKBP5 suppressed the NF-κB signaling pathway by inhibiting the nuclear translocation of NF-κB, and thereby attenuated the inflammatory response.

In conclusion, miR-23a-3p ameliorated AKI by targeting FKBP5 and NF-κB signaling in sepsis, implying a potential diagnostic or therapeutic target for AKI. Nevertheless, the pathology of sepsis is complex and the mechanism of miR-23a-3p warrants further investigation.

## CRediT authorship contribution statement

**Hui Xu:** Conceptualization, Data curation, Formal analysis, Funding acquisition, Investigation, Methodology, Project administration, Resources, Software, Supervision, Validation, Visualization, Writing – original draft, Writing – review & editing. **Zenggeng Wang:** Conceptualization, Data curation, Formal analysis, Funding acquisition, Investigation, Methodology, Project administration, Resources, Software, Supervision, Validation, Visualization, Writing – original draft, Writing – review & editing.

## Declaration of Competing Interest

The authors declare that they have no known competing financial interests or personal relationships that could have appeared to influence the work reported in this paper.

*Acknowledgements*

Not applicable.

*Funding*

The present study was supported by the Science and Technology Plan Project Program of Jiangxi Provincial Health Commission (no. 20203064).

## Appendix A. Supplementary material

Supplementary data to this article can be found online at https://doi.org/10.1016/j.cyto.2022.155898.

## References

[1] L.M. Napolitano, Sepsis 2018: Definitions and guideline changes, Surgical Infect. 19 (2) (2018) 117–125.
[2] J. Rello, F. Valenzuela-Sanchez, M. Ruiz-Rodriguez, S. Moyano, Sepsis: a review of advances in management, Adv. Ther. 34 (11) (2017) 2393–2411.
[3] M.D. Zilberberg, A.F. Shorr, S.T. Micek, M.H. Kollef, Risk factors for 30-day readmission among patients with culture-positive severe sepsis and septic shock: A retrospective cohort study, J. Hospital Med. 10 (10) (2015) 678–685.
[4] J.R. Prowle, Sepsis-associated AKI, Clin. J. Am. Soc. Nephrol.: CJASN 13 (2) (2018) 339–342.
[5] R. Bellomo, J.A. Kellum, C. Ronco, R. Wald, J. Martensson, M. Maiden, S. M. Bagshaw, N.J. Glassford, Y. Lankadeva, S.T. Vaara, A. Schneider, Acute kidney injury in sepsis, Intensive Care Med. 43 (6) (2017) 816–828.
[6] M. Godin, P. Murray, R.L. Mehta, Clinical approach to the patient with AKI and sepsis, Semin. Nephrol. 35 (1) (2015) 12–22.
[7] J. Beermann, M.T. Piccoli, J. Viereck, T. Thum, Non-coding RNAs in development and disease: background, mechanisms, and therapeutic approaches, Physiol. Rev. 96 (4) (2016) 1297–1325.
[8] A. Mohr, J. Mott, Overview of microRNA biology, Semin. Liver Dis. 35 (01) (2015) 003–11.
[9] T.X. Lu, M.E. Rothenberg, MicroRNA, J. Allergy Clin. Immunol. 141 (4) (2018) 1202–1207.
[10] N. Iwamoto, S. Fukui, A. Takatani, T. Shimizu, M. Umeda, A. Nishino, T. Igawa, T. Koga, S.Y. Kawashiri, K. Ichinose, M. Tmai, H. Nakamura, T. Origuchi, K. Chiba, M. Osaki, A. Jungel, S. Gay, A. Kawakami, Osteogenic differentiation of fibroblast-like synovial cells in rheumatoid arthritis is induced by microRNA-218 through a ROBO/Slit pathway, Arthritis Res. Ther. 20 (1) (2018) 189.
[11] J. Liu, L. Fan, H. Yu, J. Zhang, Y. He, D. Feng, F. Wang, X. Li, Q. Liu, Y. Li, Z. Guo, B. Gao, W. Wei, H. Wang, G. Sun, Endoplasmic reticulum stress causes liver cancer cells to release Exosomal miR-23a-3p and up-regulate programmed death ligand 1 expression in macrophages, Hepatology (Baltimore Md.) 70 (1) (2019) 241–258.
[12] M.S. Ostenfeld, S.G. Jensen, D.K. Jeppesen, L.-L. Christensen, S.B. Thorsen, J. Stenvang, M.L. Hvam, A. Thomsen, P. Mouritzen, M.H. Rasmussen, H.J. Nielsen, T.F. Ørntoft, C.L. Andersen, miRNA profiling of circulating EpCAM(+) extracellular vesicles: promising biomarkers of colorectal cancer, J. Extracellular Vesicl. 5 (1) (2016) 31488, https://doi.org/10.3402/jev.v5.31488.
[13] J. Lozano-Bartolomé, G. Llauradó, M. Portero-Otin, A. Altuna-Coy, G. Rojo-Martínez, J. Vendrell, R. Jorba, E. Rodríguez-Gallego, M.R. Chacón, Altered Expression of miR-181a-5p and miR-23a-3p Is Associated With Obesity and TNFα-Induced Insulin Resistance, J. Clin. Endocrinol. Metabol. 103 (4) (2018) 1447–1458.
[14] Z. Li, R. Xu, X. Zhu, Y. Li, Y.i. Wang, W. Xu, MicroRNA-23a-3p improves traumatic brain injury through modulating the neurological apoptosis and inflammation response in mice, Cell cycle (Georgetown, Tex.) 19 (1) (2020) 24–38.
[15] E. Ragni, C. Perucca Orfei, P. De Luca, A. Colombini, M. Viganò, G. Lugano, V. Bollati, L. de Girolamo, Identification of miRNA reference genes in extracellular vesicles from adipose derived mesenchymal stem cells for studying osteoarthritis, Int. J. Mol. Sci. 20 (5) (2019) 1108, https://doi.org/10.3390/ijms20051108.
[16] Q.M. Ge, C.M. Huang, X.Y. Zhu, F. Bian, S.M. Pan, Differentially expressed miRNAs in sepsis-induced acute kidney injury target oxidative stress and mitochondrial dysfunction pathways, PloS one 12 (3) (2017), e0173292.
[17] V.L. Willour, H. Chen, J. Toolan, P. Belmonte, D.J. Cutler, F.S. Goes, P.P. Zandi, R. S. Lee, D.F. MacKinnon, F.M. Mondimore, B. Schweizer, J.R. DePaulo, E. S. Gershon, F.J. McMahon, J.B. Potash, Family-based association of FKBP5 in bipolar disorder, Mol. Psychiatry 14 (3) (2009) 261–268.
[18] M. U, L. Shen, T. Oshida, J. Miyauchi, M. Yamada, T. Miyashita, Identification of novel direct transcriptional targets of glucocorticoid receptor, Leukemia 18 (11) (2004) 1850–1856.
[19] F.T. Yaylaci, D. Cicchetti, F.A. Rogosch, O. Bulut, S.R. Hetzel, The interactive effects of child maltreatment and the FK506 binding protein 5 gene (FKBP5) on dissociative symptoms in adolescence, Dev. Psychopathol. 29 (3) (2017) 1105–1117.
[20] L. Tozzi, A. Carballedo, F. Wetterling, H. McCarthy, V. O'Keane, M. Gill, D. Morris, C. Fahey, J. Meaney, T. Frodl, Single-nucleotide polymorphism of the FKBP5 gene and childhood maltreatment as predictors of structural changes in brain areas involved in emotional processing in depression, Neuropsychopharmacol.: Off. Publ. Am. College Neuropsychopharm. 41 (2) (2016) 487–497.
[21] E.J. Rahn, M.C. Guzman-Karlsson, J. David Sweatt, Cellular, molecular, and epigenetic mechanisms in non-associative conditioning: implications for pain and memory, Neurobiol. Learn. Mem. 105 (2013) 133–150.
[22] L. Wang, FKBP51 regulation of AKT/protein kinase B phosphorylation, Curr. Opin. Pharmacol. 11 (4) (2011) 360–364.
[23] T. Kanagalingam, L. Solomon, M. Vijeyakumaran, N.S. Palikhe, H. Vliagoftis, L. Cameron, IL-2 modulates Th2 cell responses to glucocorticosteroid: A cause of persistent type 2 inflammation? Immun. Inflammation Dis. 7 (3) (2019) 112–124.
[24] M.O. Altonsy, S.K. Sasse, T.L. Phang, A.N. Gerber, Context-dependent cooperation between nuclear factor κB (NF-κB) and the glucocorticoid receptor at a TNFAIP3 intronic enhancer: a mechanism to maintain negative feedback control of inflammation, J. Biol. Chem. 289 (12) (2014) 8231–8239.
[25] Y. Ma, G. Cao, J. Li, X. Hu, J.L. Liu, Silence of lncRNA HEIH suppressed liver cancer cell growth and metastasis through miR-199a-3p/mTOR axis, J. Cell. Biochem. 120 (10) (2019) 17757–17766.
[26] Y. Zhou, W. Xu, H. Zhu, CXCL8(3–72) K11R/G31P protects against sepsis-induced acute kidney injury via NF-kappaB and JAK2/STAT3 pathway, Biol. Res. 52 (1) (2019) 29.
[27] G. Sun, W. Yang, Y. Zhang, M. Zhao, Esculentoside A ameliorates cecal ligation and puncture-induced acute kidney injury in rats, Exp. Anim. 66 (4) (2017) 303–312.
[28] F. Ding, T. You, X.D. Hou, K. Yi, X.G. Liu, P. Zhang, X.K. Wang, MiR-21 regulates pulmonary hypertension in rats via TGF-beta1/Smad2 signaling pathway, Eur. Rev. Med. Pharmacol. Sci. 23 (9) (2019) 3984–3992.
[29] F. Zhang, S. Lu, S. Jin, K. Chen, J. Li, B. Huang, Y. Cao, Lidanpaidu prescription alleviates lipopolysaccharide-induced acute kidney injury by suppressing the NF-kappaB signaling pathway, Biomed. Pharmacother. 99 (2018) 245–252.
[30] R.C. Bone, R.A. Balk, F.B. Cerra, R.P. Dellinger, A.M. Fein, W.A. Knaus, R.M. H. Schein, W.J. Sibbald, Definitions for sepsis and organ failure and guidelines for the use of innovative therapies in sepsis. The ACCP/SCCM Consensus Conference Committee. American College of Chest Physicians/Society of Critical Care Medicine, Chest 101 (6) (1992) 1644–1655.
[31] Z. Wang, Z. Chen, B. Li, B.o. Zhang, Y. Du, Y. Liu, Y. He, X. Chen, Curcumin attenuates renal interstitial fibrosis of obstructive nephropathy by suppressing epithelial-mesenchymal transition through inhibition of the TLR4/NF-κB and PI3K/AKT signalling pathways, Pharm. Biol. 58 (1) (2020) 828–837.
[32] W.J. Hubbard, M. Choudhry, M.G. Schwacha, J.D. Kerby, L.W. Rue 3rd, K.I. Bland, I.H. Chaudry, Cecal ligation and puncture, Shock (Augusta, Ga.) 24 (Suppl 1) (2005) 52–57.
[33] K.J. Livak, T.D. Schmittgen, Analysis of relative gene expression data using real-time quantitative PCR and the 2(-Delta Delta C(T)) Method, Methods (San Diego, Calif.) 25 (4) (2001) 402–408.
[34] D. Zhang, X. Qiu, J. Li, S. Zheng, L. Li, H. Zhao, MiR-23a-3p-regulated abnormal acetylation of FOXP3 induces regulatory T cell function defect in Graves' disease, Biol. Chem. 400 (5) (2019) 639–650.

[35] C. Zhao, S. Wang, Y. Zhao, F. Du, W. Wang, P. Lv, L. Qi, Long noncoding RNA NEAT1 modulates cell proliferation and apoptosis by regulating miR-23a-3p/SMC1A in acute myeloid leukemia, J. Cell. Physiol. 234 (5) (2019) 6161–6172.
[36] A.S. Zannas, M. Jia, K. Hafner, J. Baumert, T. Wiechmann, J.C. Pape, J. Arloth, M. Ködel, S. Martinelli, M. Roitman, S. Röh, A. Haehle, R.T. Emeny, S. Iurato, T. Carrillo-Roa, J. Lahti, K. Räikkönen, J.G. Eriksson, A.J. Drake, M. Waldenberger, S. Wahl, S. Kunze, S. Lucae, B. Bradley, C. Gieger, F. Hausch, A.K. Smith, K. J. Ressler, B. Müller-Myhsok, K.-H. Ladwig, T. Rein, N.C. Gassen, E.B. Binder, Epigenetic upregulation of FKBP5 by aging and stress contributes to NF-κB-driven inflammation and cardiovascular risk, PNAS 116 (23) (2019) 11370–11379.
[37] J. Koeze, F. Keus, W. Dieperink, I.C. van der Horst, J.G. Zijlstra, M. van Meurs, Incidence, timing and outcome of AKI in critically ill patients varies with the definition used and the addition of urine output criteria, BMC Nephrol. 18 (1) (2017) 70.
[38] D. Marx, J. Metzger, M. Pejchinovski, R.B. Gil, M. Frantzi, A. Latosinska, I. Belczacka, S.S. Heinzmann, H. Husi, J. Zoidakis, M. Klingele, S. Herget-Rosenthal, Proteomics and Metabolomics for AKI Diagnosis, Semin. Nephrol. 38 (1) (2018) 63–87.
[39] S.M. Sutherland, Big data and pediatric acute kidney injury: the promise of electronic health record systems, Front. Pediatr. 7 (2019) 536.
[40] S.K. Sethi, R. Chakraborty, H. Joshi, R. Raina, Renal replacement therapy in pediatric acute kidney injury, Indian J. Pediatr. 87 (8) (2020) 608–617.
[41] L. Zhang, S. He, Y. Wang, X. Zhu, W. Shao, Q. Xu, Z. Cui, miRNA-20a suppressed lipopolysaccharide-induced HK-2 cells injury via NFkappaB and ERK1/2 signaling by targeting CXCL12, Mol. Immunol. 118 (2020) 117–123.
[42] T. Pan, P. Jia, N. Chen, Y. Fang, Y. Liang, M. Guo, X. Ding, Delayed remote ischemic preconditioning confersrenoprotection against septic acute kidney injury via exosomal miR-21, Theranostics 9 (2) (2019) 405–423.
[43] T. Zhang, L. Xiang, Honokiol alleviates sepsis-induced acute kidney injury in mice by targeting the miR-218-5p/heme oxygenase-1 signaling pathway, Cell. Mol. Biol. Lett. 24 (2019) 15.
[44] F. Ding, J. Lai, Y. Gao, G. Wang, J. Shang, D. Zhang, S. Zheng, NEAT1/miR-23a-3p/KLF3: a novel regulatory axis in melanoma cancer progression, Cancer Cell Int. 19 (2019) 217.
[45] S. Agostini, R. Mancuso, G. Liuzzo, E. Bolognesi, A.S. Costa, A. Bianchi, M. Clerici, Serum miRNAs expression and SNAP-25 genotype in Alzheimer's disease, Front. Aging Neurosci. 11 (2019) 52.
[46] C.M.A. van Alem, M. Schmidbauer, S. Rong, K. Derlin, J. Schmitz, J.H. Bräsen, A. Thorenz, R. Chen, J.M. Ruben, E.M. Winter, M. Schilperoort, S. Kooijman, R. A. Lalai, J.M. Metselaar, C. Klemann, M. Meier, C. van Kooten, F. Gueler, J. I. Rotmans, Liposomal delivery improves the efficacy of prednisolone to attenuate renal inflammation in a mouse model of acute renal allograft rejection, Transplantation 104 (4) (2020) 744–753.
[47] K. Van Looveren, M. Van Boxelaere, Z. Callaerts-Vegh, C. Libert, Cognitive dysfunction in mice lacking proper glucocorticoid receptor dimerization, PLoS One 14 (12) (2019), e0226753.